JCB Article

Visualization of replication initiation and elongation in *Drosophila*

Julie M. Claycomb,[1,2] David M. MacAlpine,[2,3] James G. Evans,[1] Stephen P. Bell,[2,3] and Terry L. Orr-Weaver[1,2]

[1]Whitehead Institute for Biomedical Research, [2]Department of Biology, and [3]Howard Hughes Medical Institute, Massachusetts Institute of Technology, Cambridge, MA 02142

Chorion gene amplification in the ovaries of *Drosophila melanogaster* is a powerful system for the study of metazoan DNA replication in vivo. Using a combination of high-resolution confocal and deconvolution microscopy and quantitative realtime PCR, we found that initiation and elongation occur during separate developmental stages, thus permitting analysis of these two phases of replication in vivo. Bromodeoxyuridine, origin recognition complex, and the elongation factors minichromosome maintenance proteins (MCM)2–7 and proliferating cell nuclear antigen were precisely localized, and the DNA copy number along the third chromosome chorion amplicon was quantified during multiple developmental stages. These studies revealed that initiation takes place during stages 10B and 11 of egg chamber development, whereas only elongation of existing replication forks occurs during egg chamber stages 12 and 13. The ability to distinguish initiation from elongation makes this an outstanding model to decipher the roles of various replication factors during metazoan DNA replication. We utilized this system to demonstrate that the pre–replication complex component, double-parked protein/cell division cycle 10–dependent transcript 1, is not only necessary for proper MCM2–7 localization, but, unexpectedly, is present during elongation.

Introduction

Studies in the yeast *Saccharomyces cerevisiae* have provided insight into the mechanism and control of eukaryotic DNA replication. Yeast possess specific, well-defined origins of DNA replication onto which complexes of replication factors assemble. Generally, yeast origins are 200 bp or less and consist of an 11-bp A-T–rich autonomously replicating sequence (ARS) consensus sequence, as well as the B1 and B2 elements. The pre–replication complex (pre-RC)* assembles onto these regions during the G1 phase of the cell cycle, resulting in origins that are competent to initiate DNA replication and serving as a molecular beacon to recruit the replication fork machinery (for reviews see Bielinsky and Gerbi, 2001; Bell and Dutta, 2002).

A combination of approaches in *S. cerevisiae* has identified components of the pre-RC and the replication fork machinery (for reviews see Dutta and Bell, 1997; Bell and Dutta, 2002). The six-member origin recognition complex (ORC) was identified as a pre-RC component by its ability to bind to yeast replication origins (Bell and Stillman, 1992). ORC binds to the ARS consequence sequence and B1 elements, and then recruits the pre-RC factors cell division cycle (Cdc)6/Cdc18 and double-parked protein (DUP)/Cdt1. In turn, DUP/Cdt1 and Cdc6/Cdc18 load the hexameric minichromosome maintenance proteins (MCM)2–7 complex onto pre-RCs. MCM2–7 are necessary for initiation, but are also required for elongation and travel with replication forks (Aparicio et al., 1997; Labib et al., 2000). Furthermore, MCM4, -6, and -7 have helicase activity in vitro, suggesting that they function as the replicative helicase (Ishimi, 1997).

Once MCM2–7 are loaded, additional replication factors are recruited to origins and replication initiates. Cdc45 and Mcm10 are two other factors necessary for both initiation and elongation that travel with replication forks (Merchant et al., 1997; Aparicio et al., 1999; Tercero et al., 2000; Wohlschlegel et al., 2002). CDK and Cdc7-Dbf4 kinase activity are required for initiation, with MCM2–7 and Cdc45 as potential targets (Lei et al., 1997; Zou and Stillman, 2000). Replication fork components must also be recruited for origin firing. These include the single-stranded DNA

The online version of this article contains supplemental material.

Address correspondence to Terry L. Orr-Weaver, Whitehead Institute, Cambridge, MA 02142. Tel.: (617) 258-5245. Fax: (617) 258-9872. E-mail: weaver@wi.mit.edu

D.M. MacAlpine and J.G. Evans contributed equally to this work.

*Abbreviations used in this paper: *ACE*, amplification control element; ARS, autonomously replicating sequence; BrdU, bromodeoxyuridine; Cdc, cell division cycle protein; DUP/Cdt; double-parked protein/CDC10-dependent transcript; MCM, minichromosome maintenance protein(s); ORC, origin recognition complex; *oriβ*, origin β; PCNA, proliferating cell nuclear antigen; RC, replication complex; RF, replication factor.

Key words: DNA replication; chorion amplification; ORC; DUP/Cdt1; MCM2-7

binding protein RPA, Polα/primase, the clamp loader replication factor (RF)C; the sliding clamp proliferating cell nuclear antigen (PCNA), DPB11, and the replicative polymerases Polδ/ε (for reviews see Waga and Stillman, 1998; Bell and Dutta, 2002).

Although the pre-RC and replication fork components are structurally conserved in metazoans (Donaldson and Blow, 1999), analysis of replication initiation and elongation is limited by the lack of model replicons. Using cells and extracts from humans, *Xenopus*, or *Drosophila* pre-RCs can assemble on model templates and DNA replication can initiate in vitro, giving results consistent with the yeast paradigm of pre-RC and replication fork composition and activity (Chesnokov et al., 1999; Mendez and Stillman, 2000; Blow, 2001). However, obstacles such as multiple potential initiation sites and complex cis-regulatory sequences have hindered the progress of in vivo replication initiation studies (for reviews see DePamphilis, 1999; Bielinsky and Gerbi, 2001). In addition, a lack of genetic assays has made it difficult to study the precise localization and properties of the trans-factors necessary for replication. Thus, the available models in vertebrates have yielded information about either cis-elements or trans-factors necessary for replication, but a single system has not provided information about both.

In contrast, amplification in the Dipteran flies *Drosophila melanogaster* and *Sciara coprophila* has provided the framework to study DNA replication in which the cis-regulatory sequences are well defined and trans-acting replication factors can be examined (Calvi and Spradling, 1999; Bielinsky et al., 2001). In *Sciara*, the replication start site within an amplified salivary puff origin, *ori II/9A*, is understood at the single nucleotide level and displays similarities to the yeast ARS. Furthermore, *Drosophila* ORC has been shown to bind to an 80-bp region adjacent to this replication start site (Bielinsky et al., 2001). In *Drosophila*, amplification of the chorion gene clusters provides another powerful system for the study of metazoan DNA replication. The ovarian follicle cells, somatic cells that surround the developing oocyte, synthesize and secrete the chorion, or eggshell. In response to developmental signals at stages 9 and 10 of egg chamber development, the follicle cells end genomic DNA replication and begin to amplify several clusters of genes throughout the genome, including two clusters of chorion genes (Calvi et al., 1998).

Amplification of the chorion clusters occurs via a bidirectional replication mechanism, in which initiation occurs repeatedly from defined origins and forks progress outward to ~50 kb on either side of the origins (Spradling, 1981; Spradling and Mahowald, 1981; Osheim et al., 1988; Delidakis and Kafatos, 1989; Heck and Spradling, 1990). By stage 13 of egg chamber development, a gradient of copy number results, with the origins and chorion genes located at the central, maximally amplified region. Quantitative Southern blots detect a maximum copy level of 16–20-fold for the *X* chromosome chorion cluster, and 60–100-fold for the third chromosome chorion cluster (Spradling, 1981; Delidakis and Kafatos, 1989). P-element–mediated transformation of DNA fragments from the third chromosome cluster defined the cis-regulatory element, amplification control element (*ACE*) on third chromosome (*ACE3*), which is required for high levels of amplification and sufficient for low levels of amplification (de Cicco and Spradling, 1984; Carminati et al., 1992). Two-dimensional gel analysis demonstrated that repeated firings occur from a preferred origin, *oriβ*, ~1.5 kb downstream of *ACE3* (Delidakis and Kafatos, 1989; Heck and Spradling, 1990). Further transformation experiments showed that *ACE3* interacts with *oriβ* (Lu et al., 2001).

Genetic studies took advantage of female-sterile mutations to demonstrate an essential role for known replication factors in chorion amplification. Females mutant for *orc2*, *dbf4-like*, *mcm6*, and *dup/cdt1* lay eggs with thin or otherwise abnormal eggshells due to defects in chorion amplification (Underwood et al., 1990; Landis et al., 1997; Landis and Tower, 1999; Whittaker et al., 2000; Schwed et al., 2002).

In addition to genetic approaches, the process of chorion amplification can be visualized directly. Bromodeoxyuridine (BrdU) incorporation at amplicons can be detected throughout the amplification process, from stages 10B to 13 (Calvi et al., 1998). The replication proteins ORC2, ORC1, ORC5, DUP/Cdt1, and CDC45 localize specifically to amplicons during chorion amplification in follicle cells (Asano and Wharton, 1999; Austin et al., 1999; Royzman et al., 1999; Loebel et al., 2000; Whittaker et al., 2000). In this study, we use a cell biology approach coupled with quantitative realtime PCR to decipher the dynamics of DNA replication at the chorion loci in a developmental context. We find that all initiation at chorion origins occurs during one part of amplification, whereas in subsequent stages, only the existing replication forks elongate. We also observe that the localization pattern of several replication factors during amplification correlates with the roles of these proteins in initiation or elongation.

Results

Localization patterns of ORC2 and BrdU throughout chorion amplification

We performed high-resolution deconvolution microscopy to analyze the pattern of ORC localization with respect to BrdU incorporation at the third chromosome chorion locus throughout amplification. Previous observations showed that ORC2 localizes to amplified regions for only a portion of amplification, from egg chamber stages 10A to 11 (Royzman et al., 1999). In contrast, BrdU incorporation begins in stage 10B and persists until stage 13 of egg chamber development (Calvi et al., 1998; Royzman et al., 1999; Calvi and Spradling, 2001). These differences in localization patterns suggest that DNA replication continues in the absence of ORC2 at chorion loci; that is elongation exclusively may occur during stages 12 and 13.

When BrdU incorporation became detectable early in stage 10B follicle cell nuclei, ORC2 localized to the *X* and third chromosome chorion clusters and was coincident with BrdU (unpublished data). As stage 10B continued, ORC2 no longer localized to the *X* chromosome cluster, but persisted at the third chromosome cluster, coincident with BrdU (Fig. 1, A and B; Video 1, available at http://www.jcb.org/cgi/content/full/jcb.200207046/DC1). At this time, ORC2 was present at origin sequences, as the ORC2 signal colocalized with that of a FISH probe spanning *ACE3* and *oriβ* on the third chromosome (Fig. 1, C–E). Addi-

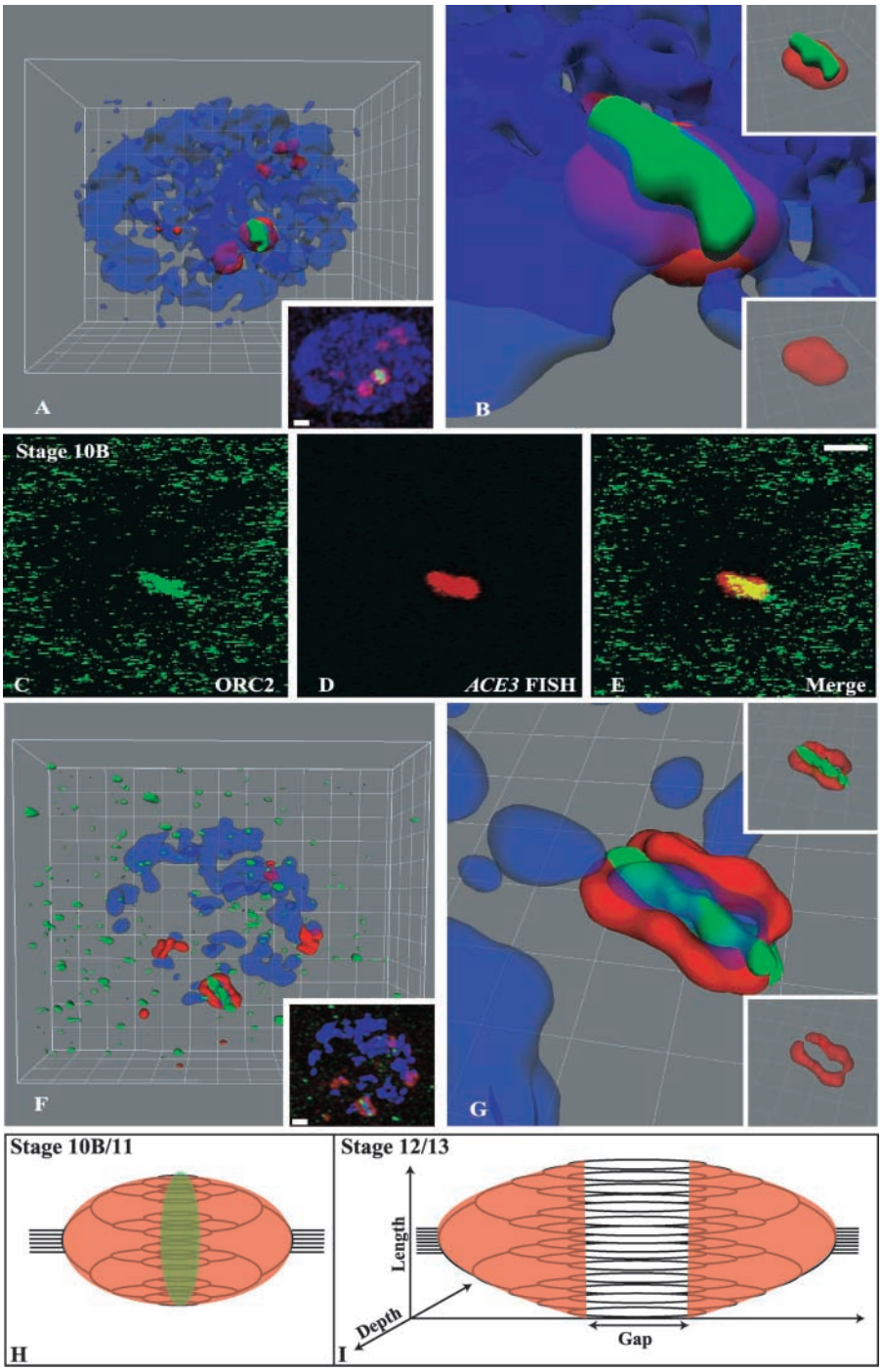

Figure 1. **ORC2 is present at chorion origins during amplification initiation but is lost from origins as initiation ends.** (A and B) Deconvolution microscopy and volume rendering shows that in stage 10B follicle cell nuclei, ORC2 (green) partially colocalizes with BrdU (red) at the third chromosome chorion cluster. DNA is in blue (TOTO). BrdU foci without ORC2 localized correspond to uncharacterized sites of amplification throughout the genome, and the focus next to the third chromosome amplicon is likely the *X* cluster. (A, inset) Immunofluorescence image from which A and B were created. (B, inset) Close-up view of BrdU and ORC2 without DNA (top), and a close-up view of BrdU only (bottom; Video 1, available at http://www.jcb.org/cgi/content/full/jcb.200207046/DC). (C–E) Confocal microscopy shows that in stage 10B follicle cell nuclei, ORC2 (green) colocalizes with FISH signal from a 3.8 kb third chromosome chorion probe (red) that spans *ACE3* and *oriβ*. (E) Shows the merged image; all images are in a single plane. (F and G) In stage 11 follicle cell nuclei, ORC2 (green) remains localized to origin regions of the third chromosome chorion locus, whereas BrdU (red) signal begins to resolve into bars as forks move outward. DNA is in blue (TOTO). (F, inset) Immunofluorescence image from which the images in F and G were created. (G, inset) Close-up view of BrdU and ORC2, without DNA (top), and a close-up view of BrdU only (bottom). (H) The onionskin/reinitiation model of chorion amplification representing the localization of ORC2 (olive) and incorporation of BrdU (salmon) in stage 10B and 11 follicle cells as initiation and limited elongation occur. (I) The onionskin/reinitiation model representing amplification by stages 12 and 13, when ORC2 is no longer localized and no further initiation events occur. Only existing replication forks move out and BrdU (salmon) incorporated at these replication forks is seen as double bars. The dimensions used for deconvolution measurements are shown in (I). Bars, 1 μm; grid boxes, 1 μm^2.

tionally, chromatin immunoprecipitation experiments have shown that in vivo, ORC is bound in the vicinity of *ACE3* and *oriβ* in amplifying stage-10 follicle cells (Austin et al., 1999). Furthermore, our observations are consistent with previous results obtained by Calvi, localizing the same FISH probe relative to BrdU incorporation (Calvi et al., 1998; Calvi and Spradling, 2001). It should also be noted that even though the follicle cells are polyploid (16C), the fact that there is a single BrdU spot (or set of double bars, see below) for each amplicon demonstrates that all the chromosome copies must be tightly aligned as polytene chromosomes (Calvi and Spradling, 2001). These data demonstrate that ORC2 is at chorion origins when they fire and begin to incorporate BrdU.

As chorion amplification proceeded, deconvolution microscopy revealed that the pattern of BrdU incorporation diverged from that of ORC2. In stage-11 egg chambers, the BrdU staining pattern resolved into a coffee bean–like structure, with bands of BrdU incorporation flanking ORC2 present at the origins (Fig. 1, F and G). Furthermore, and consistent with the results of Royzman et al. (1999), during stage 11, ORC2 dissipated from the origins and a higher level of diffuse nuclear and cytoplasmic ORC2 staining was observed. Although ORC2 staining was undetectable at

chorion loci after stage 11, BrdU incorporation continued, and during stages 12 and 13, the BrdU pattern resolved into a double bar structure (see Figs. 3 E and 4 E, BrdU and Fig. 5, C and D, lack of ORC2). Similar results were observed for ORC1 (unpublished data).

Deconvolution microscopy enabled us to measure the dimensions of the fluorescent signals at the third chromosome amplicon from stages 10B to stage 13. We examined the gap from the inside of one BrdU (or DUP, see below) signal to the inside of the second BrdU signal, the length of the bars, and the depth of each of the bars (Fig. 1 I). Based on the onionskin or reinitiation model of chorion amplification (Botchan et al., 1979; Osheim et al., 1988) (Fig 1, H and I), the gap should represent: the extent of replication fork progression; the length and number of origin firings; and the depth and complexity of the onion skin as replication forks progress outward and are arranged in three dimensions. The dimensions during stages 10B, 11, and 13 are summarized in Table I. The length of the bars remained constant after stage 11 (stage 11, 1760 nm; stage 13, 1740 nm), suggesting that the maximum number of origin firings occurred by stage 11. The depth measurement increased dramatically throughout the later stages of amplification, from 400 nm in stage 10B to 1040 nm in stage 13. The gap measurement increased from 300 nm in stage 10B to 740 nm in stage 13. The gap measurement can be used to calculate the distance in kilobases the forks have progressed at a particular stage, with the conversion factor of 100 nm $\sim$ 10 kb. This conversion factor was calculated based on data by Calvi and Spradling (2001), in which the distance of two FISH probes 46 kb apart and flanking *ACE3* was measured to be $\sim$480 nm, giving the conversion factor of 480 nm$\sim$46 kb, or $\sim$100 nm$\sim$10 kb. Thus, in stage 10B, replication forks have traveled a total distance of 30 kb (an average of 15 kb on either side of *ACE3*), and by stage 13 they have moved out across a 74-kb total region (an average of 37 kb on each side).

Considering the lack of ORC at chorion loci after stage 11, the essential role ORC plays in initiation, and the microscopy measurements, we propose that amplification can be separated into two phases. The first phase of amplification occurs during stages 10B and 11, is ORC dependent, and involves initiation coupled with elongation (Fig. 1 H). After this discrete period of initiation, ORC is lost from chorion origins and only the existing replication forks progress outward, in an elongation-only phase, to give the double bar structure seen in stages 12 and 13 (Fig. 1 I).

Table I. Deconvolution microscopy measurements of chorion amplicons

Stage	Gap	Length	Depth
		nm	
10B	300 ± 30	1280 ± 100	400 ± 50
11	550 ± 130	1760 ± 250	770 ± 100
12	740 ± 70	1740 ± 20	1040 ± 170

Measurements were made based on 10–20 follicle cell nuclei at each stage, and stained for either BrdU or DUP/Cdt1. For a more detailed description of the dimensions in reference to our model, see Fig. 1 I.

Quantitative realtime PCR measurement of DNA copy number along the third chromosome chorion amplicon

The immunofluorescence studies suggested that if the relative DNA copy number along the amplified regions were measured, a maximum copy number at origin sequences would be detected by stage 11. Furthermore, as replication forks progress outward by stages 12 and 13, we would expect to see a sequential increase in copy number of the loci proximal and distal to origins. To test this model, we used realtime PCR to quantify copy number in 5-kb intervals along the third chromosome chorion locus during each stage of egg chamber development (see Materials and methods).

Quantitation of fold amplification in each of the stages allowed us to measure both inititiation and elongation events. In stage 1–8 (preamplification) egg chambers, no amplification was observed (Fig. 2 A). Stage 10B egg chambers, in which chorion amplification has begun, showed an increase in copy number at and around *ACE3*, (from 25 to –15 kb) with a maximum of 15-fold amplification at 0 kb (Fig. 2 B). Loci proximal and distal to *ACE3*, from 25 to 35 kb and –20 to –40 kb, also showed some amplification during stage 10B (two- to fourfold). This suggests that a subset of forks had replicated the entire amplicon. By stage 11, 30-fold amplification was observed at *ACE3*, as further rounds of initiation occurred. We did not observe integral doublings of copy number at *ACE3* between stages 10B and 11, probably because pools of egg chambers were used, and the result obtained represents the average of the pool. An increase in copy number from $\sim$5 to $-$20 kb also was detected in stage 11 (Fig. 2 C).

Strikingly, in stage 12 and 13 reactions (Figs. 2, D and E, respectively), no further increase in copy number was detected at *ACE3*, with 29- and 27-fold amplification, respectively. This indicates that no further initiation occurred. In contrast, at loci proximal and distal to *ACE3*, an increase in copy number was detected as the existing replication forks progressed outward to approximately –40 and 35 kb. For example, at 35 kb, ninfold chorion amplification was detected in stage 13, and 7.5-fold chorion amplification was detected in stage 12, as compared with four and twofold in stages 11 and 10B, respectively. We observed only half the maximum level of amplification detected by Spradling's original quantitative Southern blots ($\sim$30- vs. 64-fold; Spradling, 1981), probably because of the increased sensitivity of fluorescent PCR detection and the uniformity of the intervals used to measure amplification here.

When data from all stages are compared (Fig. 2 F), it is clear that the final rounds of initiation occur between stages 10B and 11 and the copy number of flanking regions increases throughout subsequent stages. The results in Fig. 2 were obtained using the 3R nonamplified control to determine fold amplification, and similar results were observed using the *ry* control (unpublished data).

Localization patterns of PCNA and MCM2–7 during chorion amplification

Both lines of data described above indicate that initiation and elongation occur simultaneously during one phase of chorion amplification, whereas only elongation occurs dur-

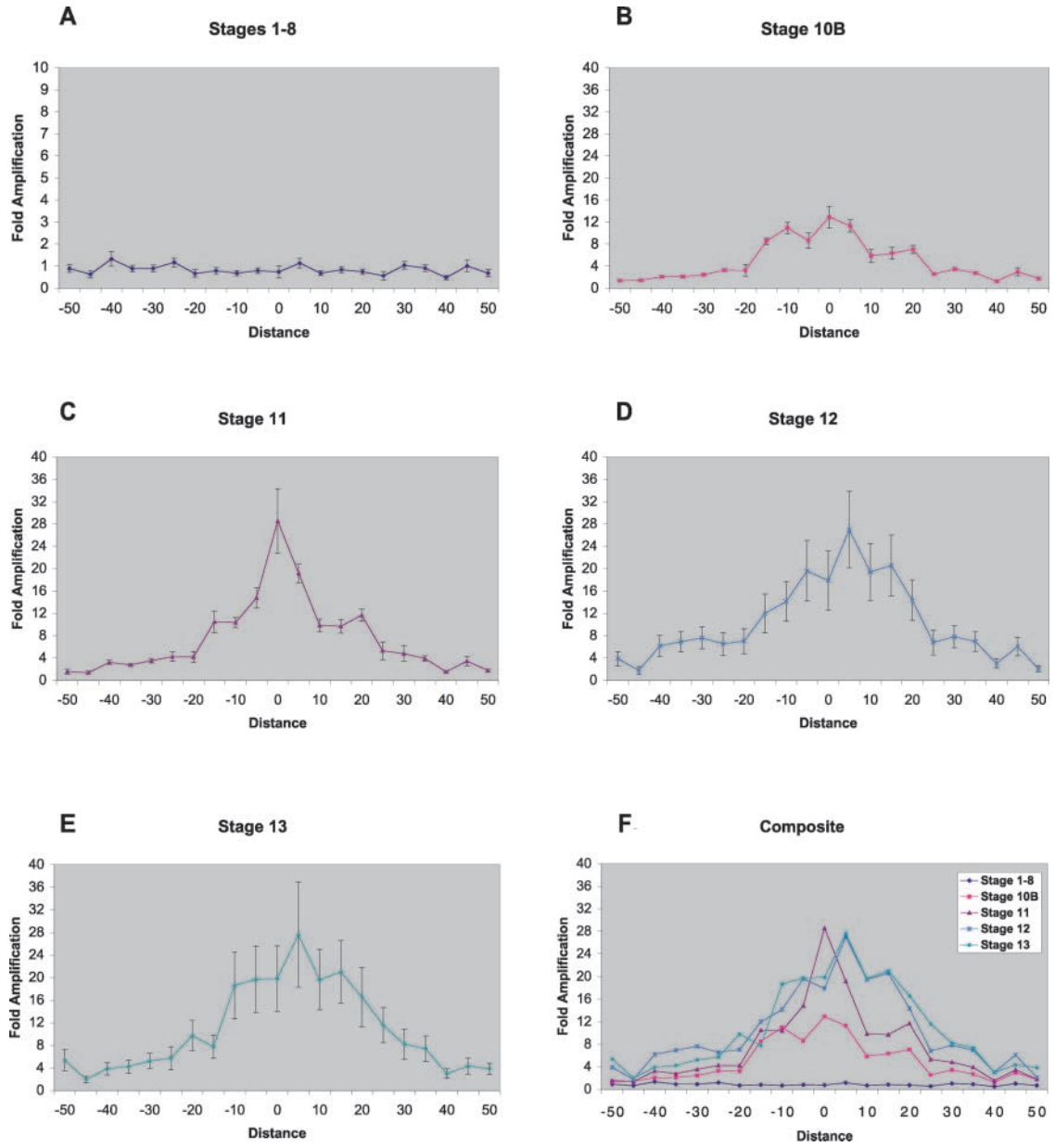

Figure 2. **Quantitative realtime PCR performed on staged egg chamber DNA confirms the timing of initiation and elongation.** DNA from egg chambers before chorion amplification, stages 1–8, and during amplification, stages 10B, 11, 12, and 13 was used in quantitative realtime PCR reactions. Primer sets used for chorion loci spanned the third chromosome 50 kb on either side of *ACE3* (denoted as 0 distance), in 5-kb intervals, and control primer sets (nonamplified) were to an intergenic region on chromosome arm *3R*. The Y axis represents fold amplification, measured as the ratio of the chorion locus to the *3R* locus and errors are the standard deviation of the sample. The X axis represents distance along the chorion locus in kilobases, with the major origin, *oriβ* located between 0 and 5 kb. (A) In stage 1–8 egg chambers, no chorion amplification has occurred and the ratio of chorion to control loci is centered at ~1. Note that the scale in A is different from the scale in B–F. (B) By stage 10B, chorion gene amplification has initiated and there is an increase in fold amplification over ~35 kb total. (C) By stage 11, additional initiation has occurred at the origins, as fold amplification increases to ~30. (D) During stage 12, no further increases in copy number are detected at origins, but an increase in fold amplification both proximal and distal to origins is detected. (E) By stage 13, replication forks have progressed out further, as an increase in fold amplification is detected out to ~35 and –40 kb. No further initiation events occurred. The stage 13 reactions were performed on two separate samples of stage 13 DNA and similar results were observed in both trials (unpublished results). (F) A composite graph of A–E showing fold amplification at the third chromosome chorion locus throughout egg chamber development.

ing a separate developmental phase. As an additional test of this hypothesis, we studied the localization patterns of replication factors known to travel with the replication forks, PCNA, and MCM2–7.

We observed a compelling pattern of PCNA localization in follicle cell nuclei. PCNA was nuclear throughout stages 1–9 (unpublished results), but by stage 10B, foci of PCNA staining were detected above faint nuclear staining (Fig. 3, A and C). As chorion amplification proceeded, PCNA remained localized and resolved into the double bar structure (Fig. 3, D and F). To ensure that PCNA was localized to chorion regions, colabeling with BrdU was performed, and PCNA was

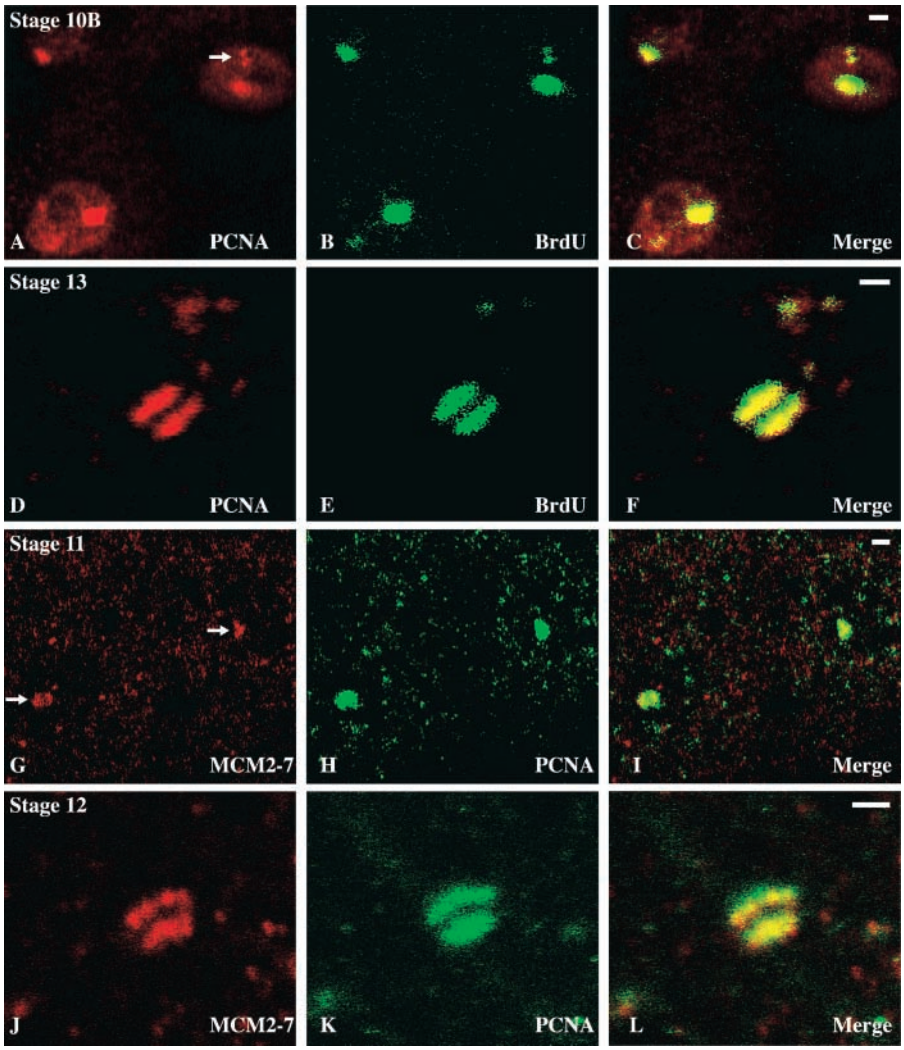

Figure 3. **PCNA and MCM2–7 staining patterns coincide with BrdU incorporation throughout amplification.** (A–C and D–F) PCNA is in red, BrdU is in green. (A–C) Several stage 10B follicle cell nuclei, in which initiation of amplification is coupled with elongation. In such nuclei, PCNA is present and colocalizes with BrdU incorporation at the *X* and the third chromosome chorion loci. The third chromosome is the larger of the foci (Calvi et al., 1998), and the *X* chromosome cluster (arrow) has already resolved into the double bar structure by this stage. In addition to being at the chorion loci, PCNA is diffusely present throughout the nucleus during this stage. (D–F) A single follicle cell nucleus from a stage 13 egg chamber shows this pattern of PCNA and BrdU staining, which is characteristic of replication fork movement. The 2 smaller foci of staining in this image may be the *X* chromosome amplicon. (G–I and J–L) MCM2–7 are in red and PCNA is in green. (G–I) MCM2–7 and PCNA colocalize in stage 11 follicle cell nuclei (arrows represent third chromosome clusters in two nuclei). (J–L) MCM2–7 staining, like PCNA, persists throughout chorion amplification and resolves into the double bar structure by stage 12. One stage 12 nucleus is shown. Bars, 1 μm.

shown to colocalize with BrdU (Fig. 3, A–C and D–F). These data support the idea that the double bar structure arises from fronts of bidirectional replication fork movement.

Previously, polyclonal antibodies raised against MCM2, -4, and -5 (Su and O'Farrell, 1997, 1998; Su et al., 1997) showed nuclear staining with no localization to chorion foci (Royzman et al., 1999). This was true even when egg chambers were treated with a high salt, high detergent buffer in an attempt to remove nonchromatin-bound MCMs from the nucleus (Schwed et al., 2002). We reexamined the localization of the MCM2–7 complex during amplification using a monoclonal antibody that recognizes an epitope present in all six *Drosophila* MCM subunits (Jayson Bowers, Anthony Schwacha, and Stephen Bell, personal communication), thereby enhancing the sensitivity of detection. Additionally, egg chambers were washed with a high salt, high detergent buffer to remove nonchromatin–bound MCM proteins from the nuclei.

Under these conditions, we saw that MCM2–7 localized throughout amplification. MCM2–7 localization first became visible as foci in stage 10B (unpublished data; Fig. 3, G and I) and progressed to the double bar structure by stages 12 and 13 (Fig. 3, J and L). To confirm that MCM2–7 were localized to the chorion regions, we costained with PCNA and observed colocalization throughout all stages of amplification (Fig. 3, G–I and J–L). Thus, MCMs are present at chorion amplicons during initiation and persist throughout amplification, presumably moving with the replication forks. The correlation of MCM2–7, PCNA, and BrdU staining patterns supports our model for chorion amplification.

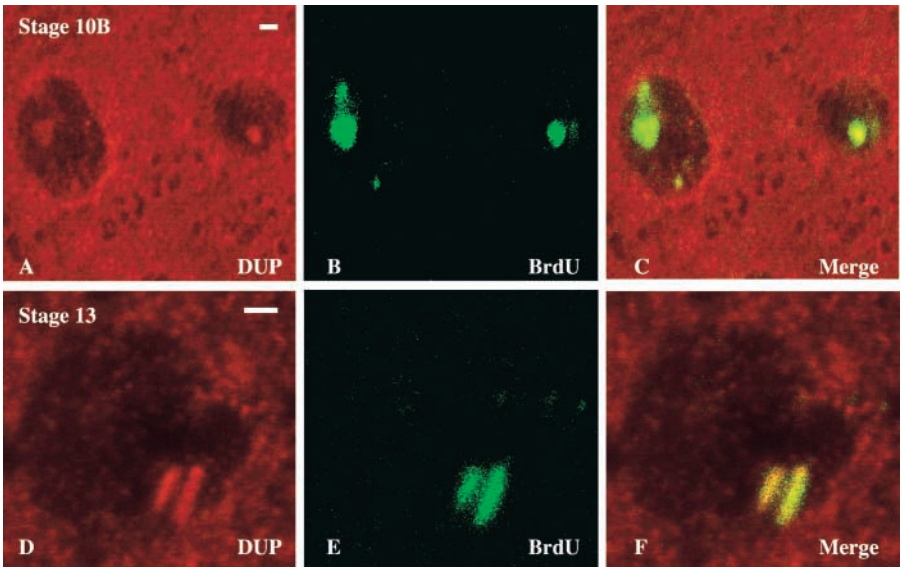

Figure 4. **DUP/Cdt1 colocalizes with BrdU throughout chorion amplification.** (A–C and D–F) DUP is in red and BrdU is in green. (A–C) In a stage 10B egg chamber, DUP colocalizes at sites of chorion amplification with BrdU. Two follicle cell nuclei are shown. (D–F) The DUP staining pattern colocalizes with that of BrdU throughout subsequent stages of chorion amplification and resolves into the double bar structure by stage 13, as seen in this follicle cell nucleus. Bars, 1 μm.

The localization pattern of DUP/Cdt1 during chorion amplification

We then characterized the properties of the pre-RC component, DUP/Cdt1 (Maiorano et al., 2000; Nishitani et al., 2000; Whittaker et al., 2000; Devault et al., 2002; Tanaka and Diffley, 2002). DUP/Cdt1 requires ORC2 to localize to chorion origins (Whittaker et al., 2000) and DUP/Cdt1 homologues in yeast and *Xenopus* have been shown to interact with Cdc6/18 to load MCM2–7 onto origins (Maiorano et al., 2000; Nishitani et al., 2000; Tada et al., 2001; Devault et al., 2002; Tanaka and Diffley, 2002). In *Xenopus* extracts, fission yeast, and budding yeast, Cdt1 is dispensable after initiation (Maiorano et al., 2000; Nishitani et al., 2000; Devault et al., 2002; Tanaka and Diffley, 2002). Furthermore, Cdt1 appears to be lost from chromatin or the nucleus at the onset of S phase (Maiorano et al., 2000; Tanaka and Diffley, 2002). These data suggest that Cdt1 is not necessary after performing its role in pre-RC formation. In contrast, the initial description of DUP/Cdt1 staining during amplification showed that DUP/Cdt1 localized to chorion loci throughout amplification, and was present during stage 13 in the double bar structure (Whittaker et al., 2000). Therefore, we examined the localization pattern of DUP/Cdt1 during amplification in relation to BrdU and ORC2, using confocal and deconvolution microscopy, to investigate whether DUP/Cdt1 could be traveling with replication forks.

DUP/Cdt1 colocalized with BrdU throughout amplification. In stage 10B, DUP/Cdt1 staining was detected as foci (Fig. 4 A) that overlapped completely with BrdU staining (Fig. 4, B and C). By stage 13, DUP/Cdt1 staining resolved into the double bar structure (Fig. 4 D) and was coincident with BrdU (Fig. 4, E and F). The fact that DUP/Cdt1 remained localized to chorion regions throughout the elongation phase suggests that DUP/Cdt1 travels with the replication forks.

We precisely localized DUP/Cdt1 with respect to ORC2 by deconvolution microscopy, and in contrast to the colocalization of DUP/Cdt1 and BrdU, the ORC2 and DUP/Cdt1 staining patterns diverged as amplification proceeded. In early stage 10B, ORC2 and DUP/Cdt1 staining overlapped (unpublished data), similar to the results with ORC2 and BrdU costaining (Fig. 1, A and B). However, by late stage 10B and stage 11, DUP/Cdt1 staining became fainter at the origins and resolved into a coffee bean–like structure (Fig. 5, A and B; Video 2, available at http://www.jcb.org/cgi/content/full/jcb.200207046/DC1). This change in the DUP/Cdt1 localization pattern occurred while ORC2 remained bound to origins. By stage 13, DUP/Cdt1 was detected in the double bar structure, with no evidence of ORC2 staining at origins (Fig. 5, C and D). Similar results were seen for DUP/Cdt1 and ORC1 (unpublished data). The pattern of DUP/Cdt1 localization in relation to BrdU and the fact that DUP/Cdt1 clears from origin sequences while ORC2 remains bound strongly indicate that DUP/Cdt1 travels with elongating replication forks.

DUP/Cdt1 is necessary to localize MCM2–7 during amplification

Given the unexpected presence of DUP/Cdt1 during elongation, we wanted to know if DUP/Cdt1 functioned in this system to load MCM2-7 during initiation. To test this, we studied the localization pattern of MCM2-7 in the dup^{PA77} female-sterile mutant ovaries. These mutants have thin eggshells and decreased and delayed BrdU incorporation during amplification (Underwood et al., 1990; Whittaker et al., 2000).

In dup^{PA77} homozygous mutant ovaries, we did not detect the localization of MCM2–7 to chorion loci at any stage of amplification (Fig. 6). Furthermore, MCM2–7 appeared to cluster at the nuclear envelope, where it colocalized with nuclear lamins. These data indicate that DUP/Cdt1 is necessary to localize MCM2–7 to origins during chorion amplification, the same as the role of DUP/Cdt1 orthologues. The clustering of MCM2–7 at the nuclear periphery suggests that DUP/Cdt1 may be necessary for the nuclear transport of MCM2–7, consistent with the findings in *S. cerevisiae* that Cdt1 and MCM2–7 display an interdependence for nuclear trafficking (Tanaka and Diffley, 2002).

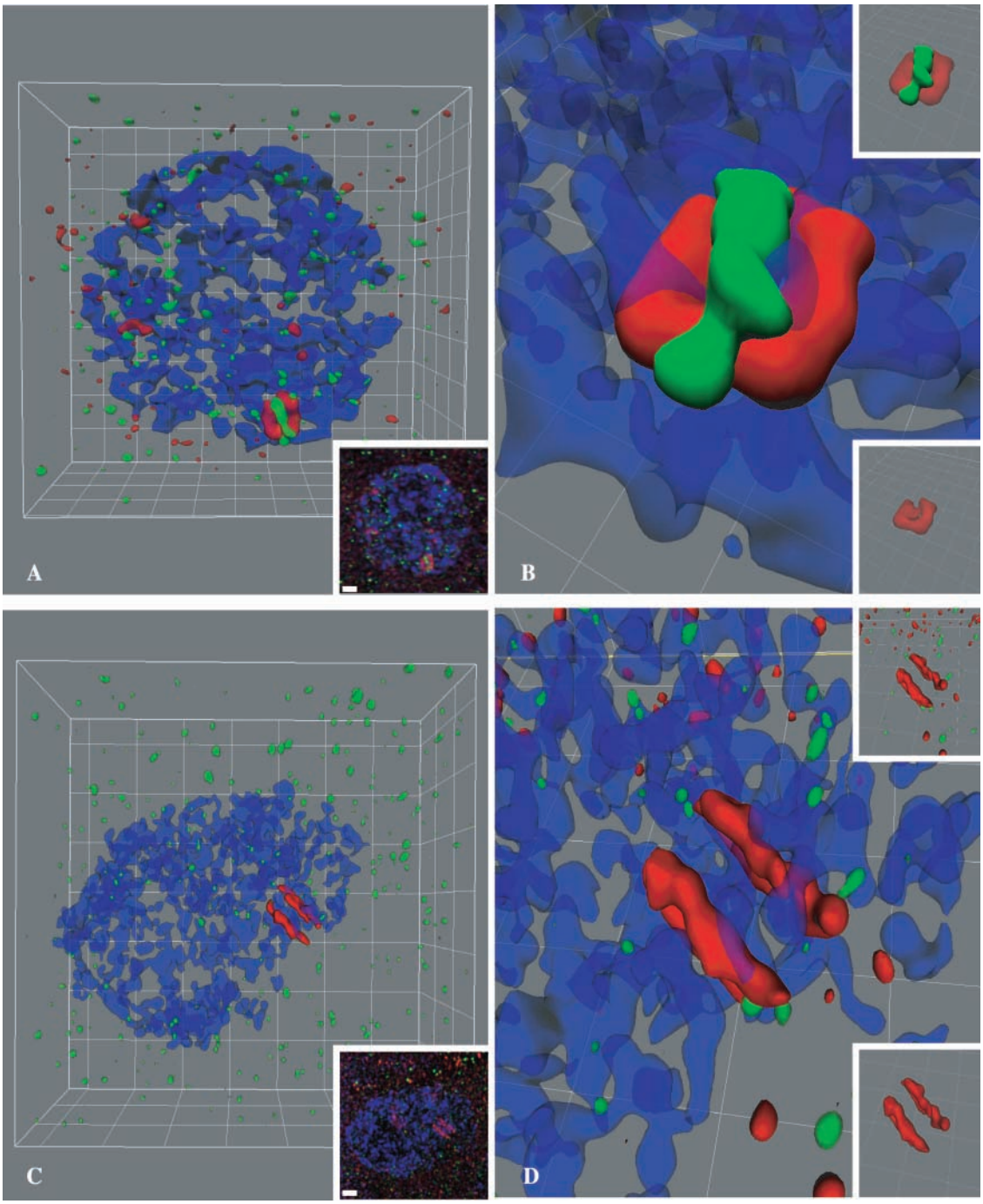

Figure 5. **The pattern of DUP and ORC2 localization indicates that DUP travels with replication forks.** (A and B) Deconvolution microscopy and volume rendering of a stage 10B follicle cell nucleus shows that the patterns of DUP/Cdt1 (red) and ORC2 (green) slightly overlap at origins. DNA is in blue (TOTO). The relative amount of DUP/Cdt1 at the origins is less than the amount of DUP/Cdt1 in regions corresponding to fronts of replication fork movement. (A, inset) Fluorescence image from which A and B were developed. (B, inset) Close-up of DUP/Cdt1 and ORC2 without the DNA (top), and a close-up view of DUP/Cdt1 alone (bottom; Video 2, available at http://www.jcb.org/cgi/content/full/jcb.200207046/DC). (C and D) By stage 13, deconvolution microscopy and volume rendering shows that ORC2 (green) has been lost from origins, whereas DUP/Cdt1 (red) persists and resolves into the double bar structure. (C, inset) Fluorescence image used to make (C and D) and the insets in (D) show a close-up view of the DUP/Cdt1 double bars in relation to ORC2 signal (top) and DUP/Cdt1 only (bottom). Bars, 1 μm; grid boxes, 1 μm^2.

Discussion

We demonstrated by three independent lines of evidence that initiation and the bulk of elongation at a chorion amplicon occur during two separate developmental periods. First, deconvolution microscopy shows that ORC and BrdU initially colocalize at origins and then diverge, as ORC is lost in stage 11 and BrdU resolves into a double bar structure. Second, elongation factors PCNA and MCM2–7 follow the same pattern as BrdU, resolving from foci early in amplification to a double bar structure by stage 12 to 13. Third,

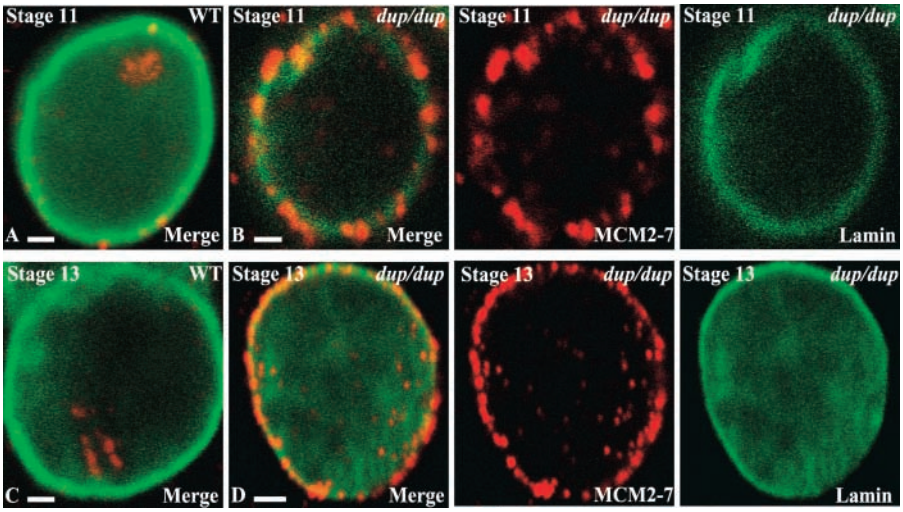

Figure 6. **MCM2–7 localization to chorion loci is disrupted in *dup*^{PA77}/*dup*^{PA77} mutants.** (A–D) MCM2–7 are in red and lamin is in green. (A and C) In wild-type follicle cells, MCM2–7 localize to chorion foci throughout the process of chorion amplification. (B and D) In contrast, in the *dup* female-sterile mutant, localization of MCM2–7 to chorion loci is not observed during any stage of amplification, and MCM2–7 cluster at the nuclear envelope. (B and D) MCM2–7 and lamin staining are shown separately to the right. At this level of resolution it is impossible distinguish whether MCM2–7 are trapped inside or outside of the nucleus. All images were captured at the same exposure for comparison. Bars, 1 μm.

quantitative realtime PCR shows a peak increase in DNA copy number at the origins by stage 11, with increases in flanking sequences becoming substantial in stages 12 and 13. Thus initiation ends by stage 11, and during stages 12 and 13 only the existing forks progress outward. Furthermore, these observations led to the unanticipated conclusion that DUP/Cdt1 travels with replication forks.

Our realtime PCR and immunofluorescence data are remarkably consistent. First, both methods restrict initiation to stages 10B and 11, and elongation to stages 12 and 13. Between stages 10B and 11, the maximum fold amplification was detected at *ACE3* by realtime PCR, ORC localized to origins, and the deconvolution showed a maximum increase in bar length. During stages 12 and 13, increases in fold amplification were detected only proximal and distal to *ACE3*, and ORC no longer localized to origins, whereas BrdU incorporation resolved into the double bar structure. Second, the distances of fork movement are consistent. Deconvolution measurements predicted that forks were maximally 30 ± 3 kb apart in stage 10B, and this correlates with the 40-kb span of peak copy number detected by realtime PCR. In stage 11, forks were measured to have progressed across a 55 ± 13-kb region by deconvolution and across a 45-kb region by realtime PCR. By stage 13, deconvolution showed that replication forks were maximally separated by 74 ± 7 kb, whereas realtime PCR measured a 75-kb span.

The convergence of the three lines of data argues against two alternative explanations for the immunofluorescence results. One alternate hypothesis is that ORC remains localized after stage 11, yet is not detectable because protein levels drop below detectable limits or epitopes become inaccessible. This is unlikely, as we observed the elongation factors PCNA, MCM2–7, and even DUP/Cdt1 change from a focus to double bar structure without a change in staining intensity. In contrast, during stage 11 ORC staining intensity decreased at origins, concomitant with a rise in nuclear and cytoplasmic levels. A second alternate hypothesis is that the double bar structures do not represent fork movement but result from firings of unidentified origins to either side of the *ACE3*/*oriβ* origin region. If this were the case, initiation events after stage 11 would occur independently of ORC, and the gradient profile from realtime PCR would be much different. As a result of these additional origins firing, the stage 12 graphs would show peaks of increased copy to either side of *ACE3*/*oriβ*, and by stage 13 the new forks would broaden the area of maximum copy number into a plateau.

The quantitative analysis of the amplification gradient provides insight into mechanisms affecting fork movement and termination and suggests that the onionskin structure (Botchan et al., 1979; Osheim et al., 1988) impedes fork movement. We calculated the maximal rate of fork movement during amplification to be 90 bp/min on average, well within the 50–100-bp/min range calculated previously (Spradling and Leys, 1988). (By quantitative realtime PCR, the furthest a replication fork could travel is 40 kb between stages 10B and 13, a period of 7.5 h.) In comparison, replication forks in the polytene larval salivary glands travel at ~300 bp/min (Steinemann, 1981), whereas rates of fork movement in both diploid *Drosophila* cell culture and embryo syncytial divisions are ~2.6 kb/min (Blumenthal et al., 1973). From these rates, it seems that polyteny hinders replication fork movement, an effect even more pronounced in amplification, given that the chorion cluster has a rate of fork movement three times less than polytene salivary glands. The fact that by stage 13 there is a gradient of copy number, and not a plateau further demonstrates the inefficiency of fork movement along the chorion cluster.

There do not seem to be specific termination sites to stop forks either along or at the ends of the chorion region, but fork movement may display some sequence or chromatin preference. The gradient of decreasing copy number implies that forks stop at a range of sites, as we would expect the presence of specific termination points along the region to cause steep drops in copy number. Despite this lack of specific termination sites, during stages 12 and 13 we see a greater increase in copy number to one side of *ACE3* (Fig. 2, graphs, right), and often observe by immunofluorescence that one of the two bars is shorter. This suggests that the sequence or chromatin structure to the other side of *ACE3* hinders fork movement, and as fewer forks move out, less BrdU incorporation occurs and a shorter bar results.

In contrast to other systems (Maiorano et al., 2000; Nishitani et al., 2000; Tada et al., 2001; Devault et al., 2002; Tanaka and Diffley, 2002), our results reveal that DUP/

Cdt1 travels with replication forks during amplification. Although it could be argued that DUP/Cdt1 simply spreads along the chromatin as amplification proceeds, this is unlikely. DUP/Cdt1 and ORC2 colocalization studies show that although ORC2 remains at origins, the DUP/Cdt1 signal decreases at origins and subsequently flanks the ORC2 signal. Furthermore, during elongation DUP/Cdt1 does not spread across the entire chorion region. Rather, there is a gap between the double bars of DUP/Cdt1 staining which increases from 300 ± 30 nm in stage 10B to 740 ± 70 nm in stage 13.

The presence of DUP/Cdt1 at forks during elongation strongly suggests it has a role in this phase of replication. Why might DUP/Cdt1 be required during elongation in this system? Chorion amplification is unique because replication forks chase forks, instead of converging as in normal eukaryotic replication. Given this peculiarity of amplification, and considering the steric constraints that arise and impede forks, DUP/Cdt1 may be necessary to maintain MCM2–7 at these lethargic forks. DUP/Cdt1 could function as a processivity factor for the MCM2–7 complex, holding it on the DNA, or it could continuously reload new MCM2–7 as they fall off the progressing replication forks. It is formally possible that although DUP/Cdt1 travels with the forks it does not perform a function. DUP/Cdt1 could simply not be expelled from the replication machinery upon initiation and then be dragged along during elongation. Although we do not favor this possibility, definitively proving that the DUP/Cdt1 at forks is necessary for elongation will require the use of a currently unavailable conditional allele. Such a mutation would permit inactivation of DUP/Cdt1 after initiation and allow a functional test for a role in elongation.

These studies highlight the complex regulation of chorion gene amplification. How are the number of origin firings restricted to the proper developmental time? It is known that the number of rounds of origin firing at the chorion amplicons is limited by the action of Rb, E2F1, and DP (Bosco et al., 2001). Perhaps DUP and MCM2–7 are also a part of this regulation, with origins firing only when MCM2–7 are properly loaded. It will also be interesting to decipher the regulation of DUP/Cdt1 during amplification. Recent studies have demonstrated that a *Drosophila* homologue of the metazoan re-replication inhibitor, Geminin, exists and interacts biochemically and genetically with DUP/Cdt1 (Quinn et al., 2001; Mihaylov et al., 2002). Female-sterile mutations in *geminin* result in increased BrdU incorporation during amplification (Quinn et al., 2001), raising the possibility that Geminin acts on DUP/Cdt1 at the chorion loci to limit origin firing. In addition to permitting the delineation of the regulatory circuitry controlling origin firing, the ability to distinguish initiation from elongation developmentally provides a powerful tool for the analysis of the properties of metazoan replication factors in vivo.

Materials and methods

Fly strains

Ovary stainings were performed on the Oregon-R wild-type strain unless otherwise noted. The *dup* mutant allele, dup^{PA77} was described previously (Underwood et al., 1990; Whittaker et al., 2000).

Immunofluorescence and BrdU labeling

Double labeling of *Drosophila* ovaries with anti-ORC2 and BrdU was performed as described previously (Royzman et al., 1999), with the following changes: BrdU was used at 6.4 μg/ml; secondary detection of ORC2 was with donkey anti–rabbit Rhodamine-RedX at 1:200; secondary detection of BrdU was with goat anti–mouse FITC at 1:200; and ovaries were mounted in Slowfade (Molecular Probes). For anti-ORC1 staining, a rat antibody obtained from Maki Asano (Duke University Medical Center, Durham, NC) was used at 1:350 and detected with donkey anti–rat Cy-3 (Jackson ImmunoResearch Laboratories) at 1:200 (Asano and Wharton, 1999).

Double labeling of *Drosophila* ovaries with anti-PCNA obtained from Daryl Henderson (SUNY at Stony Brook, Stony Brook, NY) (Henderson et al., 2000) and BrdU was performed as per anti-ORC2/BrdU, but incubating ovaries with anti-PCNA at 1:1,000 and mounting in Vectashield (Vector Labs).

Labeling of *Drosophila* ovaries with anti-MCM2–7 was performed by first washing ovaries for 30 min in high salt buffer (50 mM Hepes, pH 7.5, 100 mM NaCl, 1 mM EDTA, 0.5% Triton X-100, 0.1% Na deoxycholate), and then fixing with 8% EM grade formaldehyde, and processing as described for anti-ORC2 (Royzman et al., 1999). Ovaries were incubated with 1:200 anti-MCM2–7 overnight, and secondary detection was with donkey anti–mouse Cy-3 at 1:250. The anti-MCM2–7 is a monoclonal antibody, clone number AS1.1, which recognizes a conserved epitope in all MCM2–7 subunits, and was obtained from Jayson Bower and Anonty Schwacha (Howard Hughes Medical Institute) (Klemm and Bell, 2001). When anti-PCNA, anti-MCM2-7 costaining was performed, ovaries were treated as described for anti-MCM2–7 labeling alone, and anti-PCNA was used at 1:1,000 with anti–MCM2–7 overnight. Secondary detection of PCNA was with goat anti–rabbit FITC at 1:200, and ovaries were mounted in Vectashield. When anti-Dm_0Lamin (Gruenbaum et al., 1988), anti-MCM2–7 double labeling was performed, ovaries were treated as described, and anti-Dm_0Lamin obtained from Paul Fischer (SUNY at Stony Brook) was added at 1:200 in the primary incubation. Secondary detection of Dm_0Lamin was with goat anti–rabbit FITC at 1:150 and ovaries were mounted in Vectashield.

Double labeling of *Drosophila* ovaries with anti-DUP and BrdU was performed as per anti-ORC2/BrdU labeling (above), but incubating ovaries with anti-DUP (Whittaker et al., 2000) at 1:1,000 for 48 h at 4°C. Secondary detection of DUP was performed with donkey anti–guinea pig Rhodamine-RedX at 1:200. Slides were mounted in Vectashield.

Anti-DUP, anti-ORC2 double labeling, was performed as described previously (Whittaker et al., 2000) but with the following changes: the primary antibody incubation was performed for 48 h at 4°C, and secondary detection was with donkey anti–guinea pig Rhodamine-RedX at 1:200 for anti-DUP and goat anti–rabbit FITC at 1:200 for anti-ORC2. Ovaries were mounted in Slowfade.

For some ovary samples, TOTO (Molecular Probes) was used to stain the DNA. These samples were treated as described above, but were treated with 1 mg/ml RNase A (Sigma-Aldrich) for 1 h at room temperature, and then were incubated with a 1:2,000 dilution of TOTO (Molecular Probes) for 10 min. All secondary antibodies were from Jackson ImmunoResearch. All confocal imaging was performed using a Ziess Axiovert 100 M with LSM510 software, using 63× Plan Neofluar or 100× Plan Neofluar objectives and with filters set according to the manufacturer's parameters.

Deconvolution microscopy

Fluorescence data was collected using a Zeiss Axiovert 100 M Meta confocal microscope with LSM510 software. Excitation of FITC, rhodamine, and TOTO-1 dyes used the 488, 543, and 633 nm lasers, respectively. Emission filters were tuned to minimize bleedthrough between channels. Voxels were collected at 45 nm lateral and 1,000 nm axial intervals. Deconvolution was carried out using the cMLE algorithm of Huygens2.3-professional (Scientific Volume Imaging) on an Silicon Graphics Origin 3400 server (SGI). Rendering and analysis of three-dimensional data was carried using the MeasurementPro module of Imaris3 Surpass 3.2 (Bitplane).

Fluorescent in situ hybridization

ORC2 and *ACE3*-FISH colabeling was performed as follows. Ovaries were stained for ORC2 as described (Royzman et al., 1999). Secondary detection of ORC2 was with donkey anti–rabbit Cy3 at 1:250. After staining for ORC2, ovaries were fixed (as per the ORC2/BrdU double labeling protocol), and were then processed for whole mount FISH as described (Calvi et al., 1998). The probe used for the third chromosome chorion locus was a 3.8-kb *Sal*I fragment from the plasmid pT2, containing both *ACE3* and *oriβ*. The hybridized probe was detected with goat anti-DIG FITC at 1:200. Samples were mounted in Vectashield.

Isolation of *Drosophila* DNA for quantitative realtime PCR

Egg chamber staging was performed based on morphological markers as described (Spradling, 1993). Pools of ~400 or 500 egg chambers of each stage 10B, 11, 12, 13, and 130 ovaries of stage 1–8 were isolated from fattened Oregon-R females. DNA was isolated from the pools of egg chambers as described (Royzman et al., 1999), with the addition of RnaseA treatment (1 mg/sample; Sigma-Aldrich) during the Proteinase K step.

Embryo genomic DNA was generated for use as standard curves in the realtime PCR reactions according to standard techniques (Ashburner, 1989).

Quantitative realtime PCR

Quantitative realtime PCR was performed using the ABI Prism 7000 Sequence Detection System with QIAGEN SYBR Green PCR mix. Thermocycling was done for 35 cycles.

Primer sets spanning 50 kb on either side of *ACE3* (denoted as distance 0) at 5-kb intervals, primers to the nonamplified *rosy* (*ry*) locus, and primers to another nonamplified intergenic region on chromosome arm 3R (located approximately at cytological position 93F2, ~25 kb upstream of the *polα* locus) were generated using Primer 3 software. Primers were designed to be 22 bp on average, with an optimum Tm of 65°C, and yielding products of 85 bp on average. Primers were supplied by IDT, and primer sequences are available upon request.

Each experimental reaction (per egg chamber stage, per primer set) was performed in triplicate, alongside four tenfold dilutions of standard DNA (embryo genomic DNA) and no-template control reactions (all in triplicate). The same embryo genomic DNA samples were used in all control reactions for internal consistency. Each experimental reaction contained DNA from approximately one to one half of an egg chamber, and was done in 25 μl total volume (12.5 μl SYBR Green 2× Master Mix, 10 μl dH20, 2 μl DNA, 0.25 μl each 25 nmolar primer). Relative fluorescence was measured per sample in comparison to standard curves and standard deviations of the triplicate reactions were calculated by the ABI Prism 7000 software. Fold amplification was calculated by dividing relative fluorescence for one of the third chromosome amplicon products by the relative fluorescence of either the *ry* or the 3R non-amplified control product for a given stage. Error is expressed in terms of standard deviation, where the standard deviation of the ratio A/C = (FA/FC) *{[(SA/FA)^2 + (SC/FC)^2]^.5}. A, amplicon locus; C, control locus; FA, relative fluorescence from amplicon locus; FC, relative fluorescence from control locus (*ry* or 3R); SA, standard deviation from same amplicon locus; SC, standard deviation from same control locus.

Online supplemental material

Online supplemental materials are available at http://www.jcb.org/cgi/content/full/jcb.200207046/DC1. Video 1 accompanies Fig. 1, A and B, and shows a three-dimensional volume rendering of ORC2 (green) in relation to BrdU (red) and DNA (blue). Video 2 accompanies Fig. 5, A and B, and shows a three-dimensional volume rendering of DUP/Cdt1 (red) in relation to ORC2 (green) and DNA (blue).

We are grateful to Anthony Schwacha for supplying the monoclonal MCM2-7 antibody and to Jayson Bowers for sharing unpublished results about that antibody. We thank Paul Fisher, Daryl Henderson, and Maki Asano for donations of anti-lamin, anti-PCNA, and anti-ORC1 antibodies, respectively. We are grateful for the assistance of Milan DeVries in analyzing the realtime PCR data, and we thank Aaron Aslanian, Giovanni Bosco, Alex Ensminger, Irena Ivanovska, Gwen Wilmes, and Leah Vardy for their comments on this manuscript. The microscopy was conducted using the W.M. Keck Foundation Biological Imaging Facility at the Whitehead Institute.

D.M. MacAlpine is a fellow of the Damon Runyon-Walter Winchell Cancer Fund. This work was funded by National Institutes of Health (NIH) grant GM58701 and support from the Howard Hughes Medical Institute to S.P. Bell, and by NIH grant GM57960 to T. Orr-Weaver.

Submitted: 9 July 2002
Revised: 26 September 2002
Accepted: 26 September 2002

References

Aparicio, O.M., D.M. Weinstein, and S.P. Bell. 1997. Components and dynamics of DNA replication complexes in S. cerevisiae: redistribution of MCM proteins and Cdc45p during S phase. *Cell.* 91:59–69.

Aparicio, O.M., A.M. Stout, and S.P. Bell. 1999. Differential assembly of Cdc45p and DNA polymerases at early and late origins of DNA replication. *Proc. Natl. Acad. Sci. USA.* 96:9130–9135.

Asano, M., and R.P. Wharton. 1999. E2F mediates developmental and cell cycle regulation of ORC1 in *Drosophila*. *EMBO J.* 18:2435–2448.

Ashburner, M. 1989. *Drosophila*: A Laboratory Manual. Cold Spring Harbor Laboratory Press, Cold Spring Harbor, NY. 434 pp.

Austin, R.J., T.L. Orr-Weaver, and S.P. Bell. 1999. *Drosophila* ORC specifically binds to *ACE3*, an origin of DNA replication control element. *Genes Dev.* 13:2639–2649.

Bell, S.P., and B. Stillman. 1992. ATP-dependent recognition of eukaryotic origins of DNA replication by a multiprotein complex. *Nature.* 357:128–134.

Bell, S.P., and A. Dutta. 2002. DNA replication in eukaryotic cells. *Annu. Rev. Biochem.* 71:333–374.

Bielinsky, A.K., H. Blitzblau, E.L. Beall, M. Ezrokhi, H.S. Smith, M.R. Botchan, and S.A. Gerbi. 2001. Origin recognition complex binding to a metazoan replication origin. *Curr. Biol.* 11:1427–1431.

Bielinsky, A.K., and S.A. Gerbi. 2001. Where it all starts: eukaryotic origins of DNA replication. *J. Cell Sci.* 114:643–651.

Blow, J.J. 2001. Control of chromosomal DNA replication in the early *Xenopus* embryo. *EMBO J.* 20:3293–3297.

Blumenthal, A., H. Kriegstein, and D. Hogness. 1973. The units of DNA replication in *Drosophila melanogaster* chromosomes. *Cold Spring Harb. Symp. Quant. Biol.* 38:205–223.

Bosco, G., W. Du, and T.L. Orr-Weaver. 2001. DNA replication control through interaction of E2F-RB and the origin recognition complex. *Nat. Cell Biol.* 3:289–295.

Botchan, M., W. Topp, and J. Sambrook. 1979. Studies on simian virus 40 excision from cellular chromosomes. *Cold Spring Harb. Symp. Quant. Biol.* 43(Pt 2):709–719.

Calvi, B.R., and A.C. Spradling. 1999. Chorion gene amplification in *Drosophila*: a model for origins of DNA replication and S phase control. *In* Genetic Approaches to Eukaryotic Replication and Repair. Vol. 18. P. Fisher, editor. Academic Press, New York, New York. 407–417.

Calvi, B.R, and A. Spradling. 2001. The nuclear location and chromatin organization of active chorion amplification origins. *Chromosoma.* 110:159–172.

Calvi, B.R., M.A. Lilly, and A.C. Spradling. 1998. Cell cycle control of chorion gene amplification. *Genes Dev.* 12:734–744.

Carminati, J.L., C.J. Johnston, and T.L. Orr-Weaver. 1992. The *Drosophila* ACE3 chorion element autonomously induces amplification. *Mol. Cell. Biol.* 12: 2444–2453.

Chesnokov, I., M. Gossen, D. Remus, and M. Botchan. 1999. Assembly of functionally active *Drosophila* origin recognition complex from recombinant proteins. *Genes Dev.* 13:1289–1296.

de Cicco, D., and A. Spradling. 1984. Localization of a cis-acting element responsible for the developmentally regulated amplification of *Drosophila* chorion genes. *Cell.* 38:45–54.

Delidakis, C., and F.C. Kafatos. 1989. Amplification enhancers and replication origins in the autosomal chorion gene cluster of *Drosophila*. *EMBO J.* 8:891–901.

DePamphilis, M.L. 1999. Replication origins in metazoan chromosomes: fact or fiction. *Bioessays.* 21:5–16.

Devault, A., E.A. Vallen, T. Yuan, S. Green, A. Bensimon, and E. Schwob. 2002. Identification of Tah11/Sid2 as the ortholog of the replication licensing factor Cdt1 in *Saccharomyces cerevisiae*. *Curr. Biol.* 12:689–694.

Donaldson, A.D., and J.J. Blow. 1999. The regulation of replication origin activation. *Curr. Opin. Genet., and Dev.* 9:62–68.

Dutta, A., and S.P. Bell. 1997. Initiation of DNA replication in eukaryotic cells. *Annu. Rev. Cell Dev. Biol.* 13:293–332.

Gruenbaum, Y., Y. Landesman, B. Drees, J.W. Bare, H. Saumweber, M.R. Paddy, J.W. Sedat, D.E. Smith, B.M. Benton, and P.A. Fisher. 1988. *Drosophila* nuclear lamin precursor Dm0 is translated from either of two developmentally regulated mRNA species apparently encoded by a single gene. *J. Cell Biol.* 106:585–596.

Heck, M., and A. Spradling. 1990. Multiple replication origins are used during *Drosophila* chorion gene amplification. *J. Cell Biol.* 110:903–914.

Henderson, D.S., U.K. Wiegand, D.G. Norman, and D.M. Glover. 2000. Mutual correction of faulty PCNA subunits in temperature-sensitive lethal *mus209* mutants of *Drosophila melanogaster*. *Genetics.* 154:1721–1733.

Ishimi, Y. 1997. A DNA helicase activity is associated with an MCM4, -6, and -7 protein complex. *J. Biol. Chem.* 272:24508–24513.

Klemm, R.D., and S.P. Bell. 2001. ATP bound to the origin recognition complex is important for preRC formation. *Proc. Natl. Acad. Sci. USA.* 98:8361–8367.

Labib, K., J.A. Tercero, and J.F. Diffley. 2000. Uninterrupted MCM2-7 function

required for DNA replication fork progression. *Science.* 288:1643–1647.

Landis, G., and J. Tower. 1999. The *Drosophila chiffon* gene is required for chorion gene amplification, and is related to the yeast dbf4 regulator of DNA replication and cell cycle. *Development.* 126:4281–4293.

Landis, G., R. Kelley, A.C. Spradling, and J. Tower. 1997. The *k43* gene, required for chorion gene amplification and diploid cell chromosome replication, encodes the *Drosophila* homolog of yeast origin recognition complex subunit 2. *Proc. Natl. Acad. Sci. USA.* 94:3888–3892.

Lei, M., Y. Kawasaki, M.R. Young, M. Kihara, A. Sugino, and B.K. Tye. 1997. Mcm2 is a target of regulation by Cdc7-Dbf4 during the initiation of DNA synthesis. *Genes Dev.* 11:3365–3374.

Loebel, D., H. Huikeshoven, and S. Cotterill. 2000. Localisation of the DmCdc45 DNA replication factor in the mitotic cycle and during chorion gene amplification. *Nucleic Acids Res.* 28:3897–3903.

Lu, L., Z. Hongjun, and J. Tower. 2001. Functionally distinct, sequence specific replicator and origin elements are required for *Drosophila* chorion gene amplification. *Genes Dev.* 15:134–146.

Maiorano, D., J. Moreau, and M. Mechali. 2000. XCDT1 is required for the assembly of pre-replicative complexes in *Xenopus laevis. Nature.* 404:622–625.

Mendez, J., and B. Stillman. 2000. Chromatin association of human origin recognition complex, Cdc6, and minichromosome maintenance proteins during the cell cycle: assembly of prereplication complexes in late mitosis. *Mol. Cell. Biol.* 20:8602–8612.

Merchant, A.M., Y. Kawasaki, Y. Chen, M. Lei, and B.K. Tye. 1997. A lesion in the DNA replication initiation factor Mcm10 induces pausing of elongation forks through chromosomal replication origins in *Saccharomyces cerevisiae*. *Mol. Cell. Biol.* 17:3261–3271.

Mihaylov, I.S., T. Kondo, L. Jones, S. Ryzhikov, J. Tanaka, J. Zheng, L.A. Higa, N. Minamino, L. Cooley, and H. Zhang. 2002. Control of DNA replication and chromosome ploidy by geminin and cyclin A. *Mol. Cell. Biol.* 22:1868–1880.

Nishitani, H., Z. Lygerou, T. Nishimoto, and P. Nurse. 2000. The Cdt1 protein is required to license DNA for replication in fission yeast. *Nature.* 404:625–628.

Osheim, Y.N., O.L. Miller, and A.L. Beyer. 1988. Visualization of *Drosophila melanogaster* chorion genes undergoing amplification. *Mol. Cell. Biol.* 8:2811–2821.

Quinn, L.M., A. Herr, T.J. McGarry, and H. Richardson. 2001. The *Drosophila* Geminin homolog: roles for Geminin in limiting DNA replication, in anaphase and in neurogenesis. *Genes Dev.* 15:2741–2754.

Royzman, I., R.J. Austin, G. Bosco, S.P. Bell, and T.L. Orr-Weaver. 1999. ORC localization in *Drosophila* follicle cells and the effects of mutations in *dE2F* and *dDP. Genes Dev.* 13:827–840.

Schwed, G., N. May, Y. Pechersky, and B.R. Calvi. 2002. *Drosophila* minichromosome maintenance 6 is required for chorion gene amplification and genomic replication. *Mol. Biol. Cell.* 13:607–620.

Spradling, A.C. 1981. The organization and amplification of two clusters of *Drosophila* chorion genes. *Cell.* 27:193–202.

Spradling, A.C. 1993. Developmental genetics of oogenesis. *In* The Development of *Drosophila melanogaster*. Vol. 1. M. Bate and A. Martinez Arias, editors. Cold Spring Harbor Laboratory Press, Cold Spring Harbor, NY. 1–70.

Spradling, A.C., and E. Leys. 1988. Slow replication fork movement during *Drosophila* chorion gene amplification. *In* Cancer Cells. Vol. 6. T. Kelly and B. Stillman, editors. Cold Spring Harbor Laboratory Press, Cold Spring Harbor. 305–309.

Spradling, A.C., and A.P. Mahowald. 1981. A chromosome inversion alters the pattern of specific DNA replication in *Drosophila* follicle cells. *Cell.* 27:203–209.

Steinemann, M. 1981. Chromosomal replication in *Drosophila virilis*. III. Organization of active origins in the highly polytene salivary gland cells. *Chromosoma.* 82:289–307.

Su, T.T., and P.H. O'Farrell. 1997. Chromosome association of minichromosome maintenance proteins in *Drosophila* mitotic cycles. *J. Cell Biol.* 139:13–21.

Su, T.T., and P.H. O'Farrell. 1998. Chromosome association of minichromosome maintenance proteins in *Drosophila* endoreplication cycles. *J. Cell Biol.* 140: 451–460.

Su, T.T., N. Yakubovich, and P.H. O'Farrell. 1997. Cloning of *Drosophila* MCM homologs and analysis of their requirement during embryogenesis. *Gene.* 192:283–289.

Tada, S., A. Li, D. Maiorano, M. Mechali, and J.J. Blow. 2001. Repression of origin assembly in metaphase depends on inhibition of RLF-B/Cdt1 by geminin. *Nat. Cell Biol.* 3:107–113.

Tanaka, S., and J.F. Diffley. 2002. Interdependent nuclear accumulation of budding yeast Cdt1 and Mcm2–7 during G1 phase. *Nat. Cell Biol.* 4:198–207.

Tercero, J.A., K. Labib, and J.F. Diffley. 2000. DNA synthesis at individual replication forks requires the esential initiation factor Cdc45p. *EMBO J.* 19: 2082–2093.

Underwood, E.M., A.S. Briot, K.Z. Doll, R.L. Ludwiczak, D.C. Otteson, J. Tower, K.B. Vessey, and K. Yu. 1990. Genetics of 51D-52A, a region containing several maternal-effect genes and two maternal-specific transcripts in *Drosophila*. *Genetics.* 126:639–650.

Waga, S., and B. Stillman. 1998. The DNA replication fork in eukaryotic cells. *Annu. Rev. Biochem.* 67:721–751.

Whittaker, A.J., I. Royzman, and T.L. Orr-Weaver. 2000. *Drosophila* double parked: a conserved, essential replication protein that colocalizes with the origin recognition complex and links DNA replication with mitosis and the down-regulation of S phase transcripts. *Genes Dev.* 14:1765–1776.

Wohlschlegel, J.A., S.K. Dhar, T.A. Prokhorova, A. Dutta, and J.C. Walter. 2002. *Xenopus* Mcm10 binds to origins of DNA replication after Mcm2-7 and stimulates origin binding of Cdc45. *Mol. Cell.* 9:233–240.

Zou, L., and B. Stillman. 2000. Assembly of a complex containing Cdc45p, replication protein A, and Mcm2p at replication origins controlled by S-phase cyclin-dependent kinases and Cdc7p-Dbf4p kinase. *Mol. Cell. Biol.* 20: 3086–3096.